2021

Strained alkyne polymers capable of SPAAC via ring-opening metathesis polymerization

Rajeshwar Vasdev

Wilson Luo

Kyle Classen

Michael Anghel

Samantha Novoa

See next page for additional authors

Authors

Rajeshwar Vasdev, Wilson Luo, Kyle Classen, Michael Anghel, Samantha Novoa, Mark S. Workentin, and Joe B. Gilroy

ARTICLE

Strained alkyne polymers capable of SPAAC via ring-opening metathesis polymerization

Rajeshwar Vasdev,[a] Wilson Luo,[a] Kyle Classen,[a] Michael Anghel,[a] Samantha Novoa,[a] Mark S. Workentin,[a*] and Joe B. Gilroy [a*]

The incorporation of strained alkynes into polymers is generally achieved by employing step-growth polymerization methods or post-polymerization reactions. Here, we demonstrate that cyclopropenone-masked strained alkynes are tolerant to chain-growth ring-opening metathesis polymerization, and that, upon post-polymerization photochemical demasking with loss of CO, the strained alkyne group appended to each repeating unit can be used to prepare functional (*e.g.*, fluorescent or redox-active) polymers from a common polymer backbone. We support our claims about polymer transformations throughout the manuscript through the inclusion of a complete set of model reactions and characterization data for analogous molecular species. The findings of this study are transferable to other polymeric systems, opening the door to the creation of libraries of multifunctional chain-growth polymers with identical polymer backbones.

Introduction

The copper-assisted azide-alkyne cycloaddition (CuAAC) click reaction is now ubiquitous in organic synthesis, polymer chemistry, and materials chemistry due to its selective, high yielding, and atom economic nature.[1-3] However, despite these attractive traits, the toxicity of copper used in the CuAAC reaction has spurred the development of copper-free alternatives.[4] Strain-promoted azide-alkyne cycloaddition (SPAAC) reactions circumvent the use of copper by introducing ring strain at the alkyne and have been widely used in the chemical biology arena.[5-8]

SPAAC reactions have found application in other areas, including polymer chemistry,[9] where the absence of copper is also attractive. Examples involving azide-functionalized polymers and materials reacting with strained alkynes post-polymerization represent the most common use of SPAAC in this regard.[10-14] However, strained alkynes have been incorporated into the backbone of conjugated polymers prepared by step-growth methods,[15-17] and the SPAAC reaction has also been harnessed in bond-forming reactions for the preparation of linear and cyclic polymers.[18-21]

The impressive reactivity that renders the SPAAC reaction useful in the applications described above has also hindered the development of strained-alkyne-containing polymers produced by chain-gro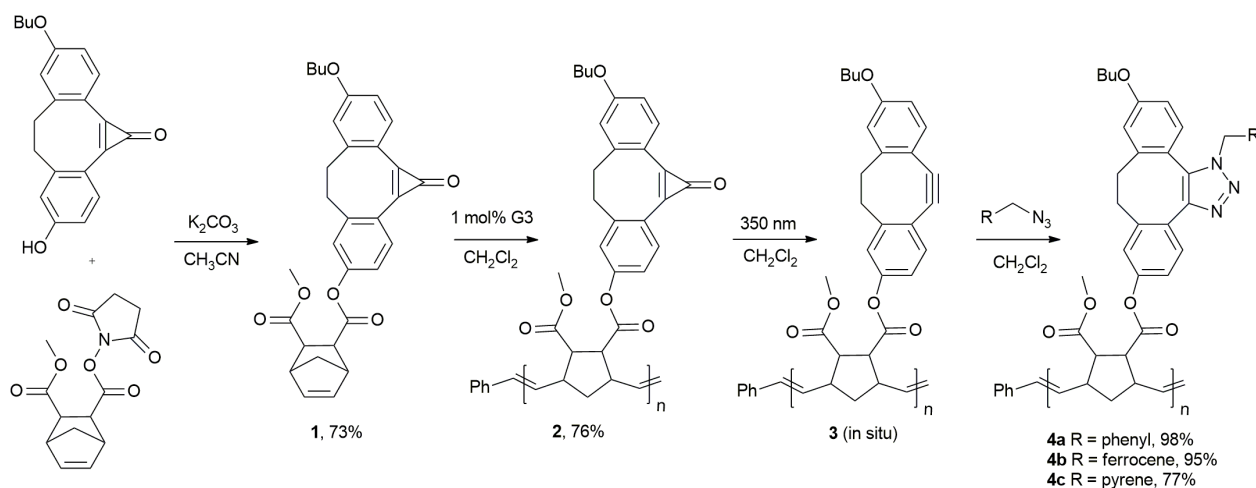wth methods, including ring-opening metathesis polymerization (ROMP), as strained alkynes polymerize under such conditions.[22-23] The photochemistry of cyclopropenones as photochemical precursors to strained alkynes has been well studied, mainly by Popik and co-workers. For dibenzocyclooctynes like the one used in this study, they showed that irradiation with 350 nm light resulted in efficient (quantum yield = 0.33) decarbonylation to yield strained alkynes quantitatively.[24] This masking-demasking strategy has led to the production of cyclic,[25-26] end-group functionalized,[27-28] H- and T-shaped,[29] and surface-grafted polymers.[30-31] However, no such strategies have been demonstrated for the production of chain-growth polymers.

Here, we present a strategy for the incorporation of cyclopropeneone-masked strained alkynes into polymers produced by ROMP and demonstrate that the strained alkyne can be liberated photochemically and then used to prepare functional polymers using copper-free SPAAC reactions. This strategy offers several attractive traits in the context of functional polymer chemistry. i) It circumvents the need for potentially dangerous polyazides to be produced. ii) It results in a strained alkyne being present on every repeating unit of the polymer backbone, thus allowing for polymers with uniform and predictable structure and properties to be reproducibly prepared. iii) The strained alkynes incorporated are readily and quantitatively functionalized in the absence of copper via post-polymerization reactions affording libraries of polymers with identical polymer backbones and different functional side chains.

Scheme 1 Synthesis and functionalization of strained-alkyne polymer **3**.

Results and Discussion

Our synthetic approach is outlined in Scheme 1 and includes analogous reactions and full characterization (NMR, IR, and UV-vis absorption spectroscopy and mass spectrometry) of molecular analogues at each step to serve as models for the polymer transformations reported here (see supplementary information). The first step involved the combination of the alcohol-functionalized, cyclopropenone-masked dibenzocyclooctyne previously reported by Locklin and co-workers[30] and the succinimide-activated derivative of *endo*-monomethyl-5-norbornene-2,3-dicarboxylate (Fig. S1–S3) to produce monomer **1** in 73% yield (Fig. S4–S7). ROMP of monomer **1** to produce a sample of polymer **2** (76% yield, M_n = 41,640 g mol^{-1}, Đ = 2.09) bearing cyclopropenone-masked dibenzocyclooctyne groups for analysis and further reactivity was accomplished using 1 mol% of the 3-bromopyridine derivative of Grubbs 3rd generation catalyst (G3) in CH$_2$Cl$_2$ at 25 °C (Fig. S8–S11). The IR spectra of **1** and **2** were a qualitative match, with broadening observed in the case of the polymer. The characteristic carbonyl absorption associated with the cyclopropenone group at 1842 cm^{-1} was present in both spectra. The ^{1}H NMR spectra of **1** and **2** were also similar (Fig. 1), with broadening observed in the spectrum collected for the polymer. The alkene protons of the norbornene group shifted from 6.45 and 6.25 ppm in the spectrum of monomer **1** to 5.74 and 5.52 ppm in the spectrum of polymer **2** while other signals
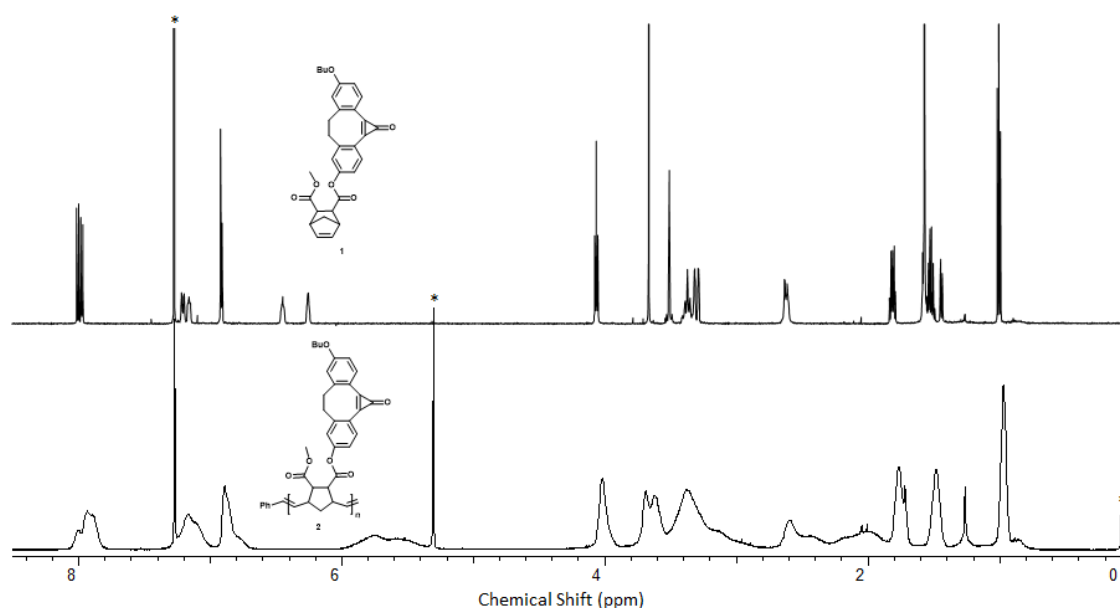

Fig. 1 ^{1}H NMR spectra of cyclopropenone-masked monomer **1** (top) and polymer **2** (bottom) in CDCl$_3$. Asterisks denote residual CHCl$_3$, CH$_2$Cl$_2$, and grease.
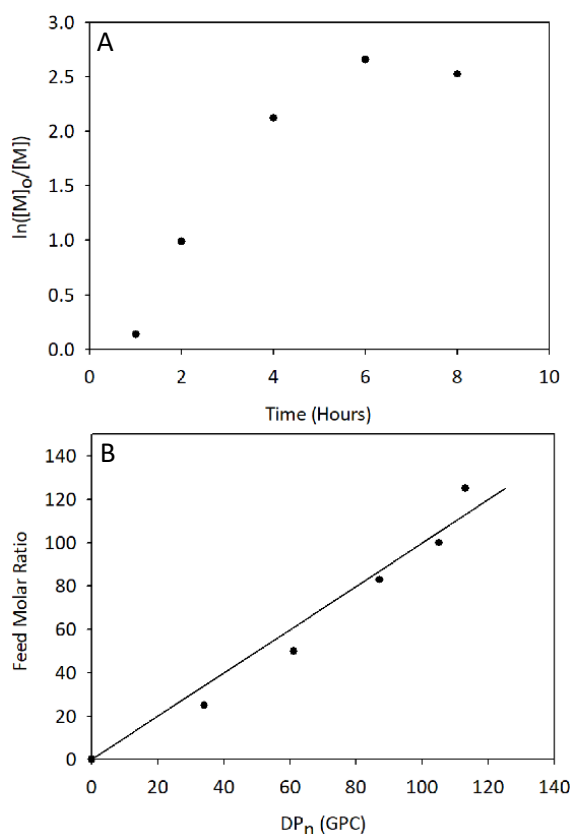
Fig. 2 A) Semilogarithmic plot and B) relationship between feed molar ratio and DP_n for the conversion of monomer **1** to polymer **2** using G3 in CH_2Cl_2. GPC traces corresponding to panel A) are shown in Fig. S14.

Table 1 Molecular weight data as a function of time for the ROMP of monomer **1** with 1 mol% of G3 in CH_2Cl_2. Corresponding GPC traces are shown in Fig. S14.[a]

time (h)	M_n (g mol^{-1})	M_w (g mol^{-1})	Đ
1	30,100	52,250	1.74
2	53,550	86,650	1.62
4	60,500	100,300	1.70
6	59,900	121,500	2.03
8	59,700	117,400	2.00

[a]GPC experiments were conducted in DMF containing 10 mM LiBr and 1% NEt and molecular weights are relative to polystyrene standards.

remained unchanged apart from broadening. Polymer **2** showed thermal stability up to a temperature of 240 °C before it gradually lost mass in two steps when studied by thermal gravimetric analysis (TGA, Fig. S12). Differential scanning calorimetry (DSC) revealed a glass transition at 172 °C (Fig. S13). We probed the ROMP reaction of monomer **1** in detail, including studies of molecular weight and monomer consumption as a function of time (Table 1, Fig. 2 and S14). In all cases, at the early stages of polymerization where the concentration of monomer was high, characteristics typical of living ROMP were observed. However, as the reactions proceeded, deviation from ideal behaviour was observed, likely because of side reactions involving either the cyclopropenone functional group or the alkene groups of the backbone as the concentration of strained alkenes associated with the monomer diminished. It should be noted that these side reactions were very minor as we were unable to detect the products of such
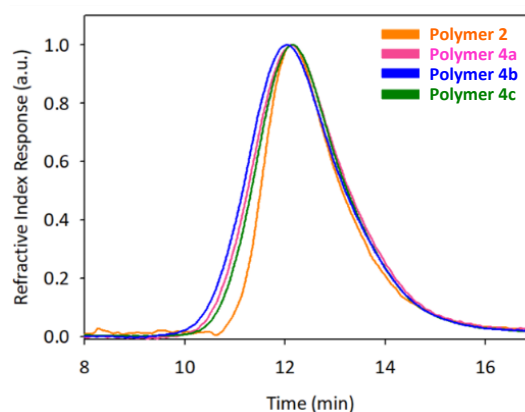

Fig. 3 GPC Traces (DMF vs. polystyrene standards) for polymers **2** and **4a–c**.

side reactions using common spectroscopy techniques. Importantly, the ROMP of monomer **1** offered good control over molecular weight (Fig. 2), a trait that remains elusive for step-growth polymerization reactions used to produce strained alkyne polymers. To probe the possible side reactions, a model cyclopropenone-masked dibenzocyclooctyne without the polymerizable norbornene group was exposed to the same G3 catalyst and conditions. There was no measurable reactivity over the same timescale, and all starting material was recovered suggesting that the side reactions were likely not due to the strained alkene moiety of the cyclopropenone.

Irradiation of polymer **2** with 350 nm light in CH_2Cl_2 using a procedure like that developed by Popik and co-workers[24, 32] resulted in loss of CO from the cyclopropenone group to liberate the strained alkyne polymer **3** in 99% yield (Fig. S8, S15−S19). Photochemical demasking of the strained alkyne group resulted in a shift in the CH resonances of the benzene rings attributed to the dibenzocyclooctyne units in the respective ^{1}H NMR spectra of polymers **2** and **3**. Perhaps more diagnostic are the UV-Vis absorption spectra obtained for **2** and **3** (Fig. S7 and S8). The cyclopropenone-masked polymer showed two broad absorption maxima at 323 and 342 nm that blue-shifted upon demasking to 304 and 320 nm.[33] IR spectroscopy also indicated that the cyclopropenone group had been cleanly removed from polymer **2** (compare Fig. S10 and S19). For each spectroscopic characterization method employed, signals corresponding to polymer **2** were not detected upon demasking.

In our hands, polymer **3** was stable for at least several hours in solution and several days in the solid-state at −20 °C, allowing for its characterization. However, given that the photo-demasking reaction is quantitative and produces only CO gas as a by-product, we chose to generate it *in situ* prior to reaction with a slight excess of a range of azides to produce functionalized polymers **4a–c** via a metal-free SPAAC reaction in a single pot (Scheme 1). The cycloaddition leads, in principle, to two regioisomers of the triazole; only one is shown for simplicity. In each case, the SPAAC reaction was accompanied by the disappearance of the absorption bands centred at 304 and 320 nm attributed to the dibenzocyclooctyne units in the respective UV-Vis absorption spectra (Fig. S7 and S8) and the disappearance of stretches associated with the azide and
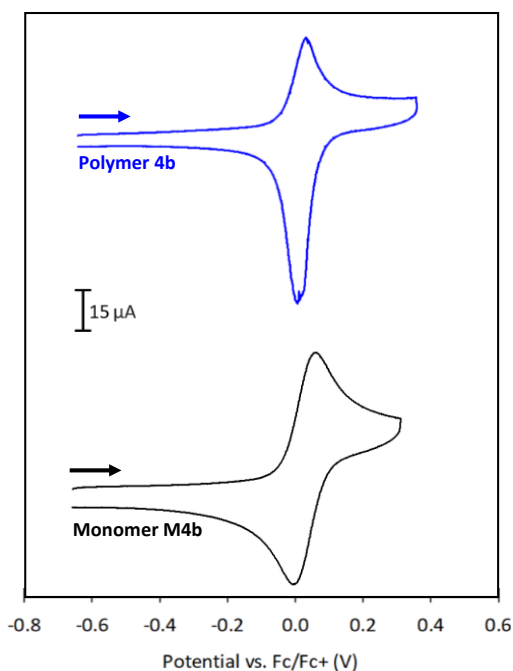
Fig. 4 Cyclic voltammograms of ferrocene-functionalized polymer **4b** and monomer **M4b** collected in dry, degassed CH_2Cl_2 containing ~1 mM analyte and 0.1 M [nBu$_4$N][PF$_6$] as supporting electrolyte at a scan rate of 250 mV s^{-1}.
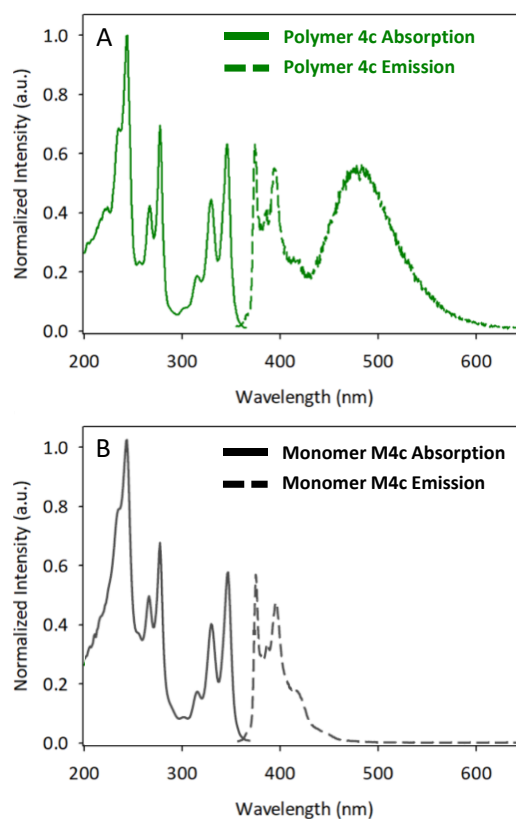

Fig. 5 UV-vis absorption (solid lines) and emission (dashed lines) spectra of A) pyrene-functionalized polymer **4c** and B) pyrene-functionalized monomer **M4c** recorded in degassed CH_2Cl_2 at a concentration of 1×10^{-6} M.

strained alkyne functional groups in the respective FT-IR spectra. The related NMR spectra did not show signals that could be assigned to the masked or free strained alkyne.

Benzyl-functionalized derivative **4a** (Fig. S7, S8, S20–S26; M_n = 44,780 g mol^{-1}, Đ = 2.43) served as a model polymer, while ferrocene- and pyrene-functionalized polymers **4b** (Fig. S27–S35; M_n = 50,890 g mol^{-1}, Đ = 2.17) and **4c** (Fig. S36–S42; M_n = 33,710 g mol^{-1}, Đ = 2.52) demonstrated, as a proof of concept, that redox-active and emissive polymers could be prepared using our strategy. Fig. 3 shows the GPC traces collected for polymers **2** and **4a–c** and demonstrates that the molecular weight distribution of the polymers does not change significantly and no high- or low-molecular weight shoulders are present, as would be expected due to their common origin from polymer **3** via the efficient and selective SPAAC reaction. Slight differences in molecular weights and modest broadening of the molecular weight distributions are likely due to changes in polymer morphology and/or polymer-column interactions associated with the benzyl-, ferrocene-, and pyrene-functionalized polymers, which each have unique solubilities and polarities.

TGA of benzyl-functionalized polymer **4a** led to thermal degradation in two steps and an earlier onset of decomposition (195 °C) when compared to the cyclopropenone-masked polymer. DSC analysis did not lead to observation of a glass transition within the thermal stability window of the polymer.

Ferrocene-functionalized polymer **4b** gave rise to a weak absorption at *ca.* 450 nm in its UV-Vis absorption spectrum because of a Laporte-forbidden d→d transition (Fig. S31) and showed enhanced thermal stability, relative to polymers **2** and **4a**, with an onset of decomposition of 315 °C. No glass

transition was detected below the degradation point. The ferrocene groups appended to each repeating unit of the polymer backbone also imparted redox activity. Cyclic voltammetry studies of polymer **4b** in CH_2Cl_2 showed that it was electrochemically converted to its corresponding polycation at an oxidation potential of 0.02 V relative to the ferrocene/ferrocenium redox couple (Fig. 4). The enhanced current response observed on the anodic sweep points to a loss of diffusion control at the working electrode interface associated with the diminished solubility of the polycation. A reversible oxidation wave was observed for the monomeric analogue **M4b** (Fig. 4).

Polymer **4c**, which includes pyrene units appended to its polymer backbone, showed an onset of thermal decomposition at 265 °C and no glass transition within its window of stability. The incorporation of pyrene imparted the expected absorption properties for pyrene moiety (Fig. 5). Absorption bands centred at 244, 267, 315, 330, and 346 nm were observed for polymer **4c** and its monomeric analogue **M4c**. Similarly, emission bands typical of pyrene were observed for both species at *ca.* 373, 384, and 394 nm.[34] However, in the case of polymer **4c**, an additional broad emission band centred at 479 nm was observed (Fig. 5). This band was not observed for the monomeric analogue of **4c** and can be attributed to pyrene excimer formation[35] as a result of the close proximity of the pyrene units within the polymeric construct produced by SPAAC.

Conclusions

In this paper, we describe the first successful chain-growth polymerization strategy to produce strained alkyne polymers. Cyclopropenone-masked strained alkynes were polymerized using ROMP affording polymers that could be produced with good control over their molecular weights and limited side reactions when the concentration of monomer was appreciable. Facile photochemical demasking of the strained alkyne groups in each repeating unit afforded a polymer that underwent efficient SPAAC with several model functional azides to yield benzyl-, ferrocene-, and pyrene-functionalized polymers from a common backbone. In executing this project, we have opened the door to routes to produce a wide range of strained alkyne polymers via chain-growth polymerization reactions that can be further modified to tune their properties, adding a new dimension to the use of SPAAC chemistry in the polymer sciences.

Conflicts of interest

There are no conflicts to declare.

Acknowledgements

Notes and references

1 L. Liang and D. Astruc, *Coord. Chem. Rev.*, 2011, **255**, 2933–2945.
2 E. Haldón, M. C. Nicasio and P. J. Pérez, *Org. Biomol. Chem.*, 2015, **13**, 9528–9550.
3 S. Neumann, M. Biewend, S. Rana and W. H. Binder, *Macromol. Rapid. Commun.*, 2020, **41**, 1900359.
4 N. Z. Fantoni, A. H. El-Sageer and T. Brown, *Chem. Rev.*, 2021, **121**, 7122–7154.
5 N. J. Agard, J. M. Baskin, J. A. Prescher, A. Lo and C. R. Bertozzi, *ACS Chem. Biol.*, 2006, **1**, 644–648.
6 J. C. Jewett and C. R. Bertozzi, *Chem. Soc. Rev.*, 2010, **39**, 1272–1279.
7 C. P. Ramil and Q. Lin, *Chem. Commun.*, 2013, **49**, 11007–11022.
8 C. J. Pickens, S. N. Johnson, M. M. Pressnall, M. A. Leon and C. J. Berkland, *Bioconjugate Chem.*, 2018, **29**, 686–701.
9 K. Li, D. Fong, E. Meichsner and A. Adronov, *Chem. Eur. J.*, 2021, **27**, 5057–5073.
10 J. Xu, F. Prifti and J. Song, *Macromolecules*, 2011, **44**, 2660–2667.
11 P. A. Ledin, N. Kolishetti and G. J. Boons, *Macromolecules*, 2013, **46**, 7759–7768.
12 S. Hackelbusch, T. Rossow, H. Becker and S. Seiffert, *Macromolecules*, 2014, **47**, 4028–4036.
13 D. Fong, G. M. Andrews, S. A. McNelles and A. Adronov, *Polym. Chem.*, 2018, **9**, 4460–4467.
14 A. Uvyn, R. De Coen, O. De Wever, K. Deswarte, B. N. Lambrecht and B. G. De Geest, *Chem. Commun.*, 2019, **55**, 10952–10955.
15 V. Kardelis, R. C. Chadwick and A. Adronov, *Angew. Chem. Int. Ed.*, 2016, **55**, 945–949.
16 V. Kardelis, K. Li, I. Nierengarten, M. Holler, J.-F. Nierengarten and A. Adronov, *Macromolecules*, 2017, **50**, 9144–9150.
17 K. Li, V. Kardelis and A. Adronov, *J. Polym. Sci., Part A: Polym. Chem.*, 2018, **56**, 2053–2058.
18 J.-Q. Chen, L. Xiang, X. Liu, X. Liu and K. Zhang, *Macromolecules*, 2017, **50**, 5790–5797.
19 L. Qu, P. Sun, Y. Wu, K. Zhang and Z. Liu, *Macromol. Rapid. Commun.*, 2017, **38**, 1700121.
20 P. Sun, J. Chen, J. Liu and K. Zhang, *Macromolecules*, 2017, **50**, 1463–1472.
21 L. Xiang, Z. Li, J. Liu, J. Chen, M. Zhang, Y. Wu and K. Zhang, *Polym. Chem.*, 2018, **9**, 4036–4043.
22 F. R. Fischer and C. Nuckolls, *Angew. Chem. Int. Ed.*, 2010, **49**, 7257–7260.
23 D. E. Bellone, J. Bours, E. H. Menke and F. R. Fischer, *J. Am. Chem. Soc.*, 2015, **137**, 850–856.
24 A. A. Poloukhtine, N. E. Mbua, M. A. Wolfert, G.-J. Boons and V. V. Popik, *J. Am. Chem. Soc.*, 2009, **131**, 15769–15776.
25 P. Sun, Q. Tang, Z. Wang, Y. Zhao and K. Zhang, *Polym. Chem.*, 2015, **6**, 4096–4101.
26 Q. Tang, J. Chen, Y. Zhao and K. Zhang, *Polym. Chem.*, 2015, **6**, 6659–6663.
27 P. Sun, G. Yan, Q. Tang, Y. Chen and K. Zhang, *Polymer*, 2015, **64**, 202–209.
28 L. Qu, Y. Wu, P. Sun, K. Zhang and Z. Liu, *Polymer*, 2017, **114**, 36–43.
29 W. Zhu, Z. Li, P. Sun, L. Ren and K. Zhang, *Polymer*, 2016, **86**, 1–7.
30 R. M. Arnold, C. D. McNitt, V. V. Popik and J. Locklin, *Chem. Commun.*, 2014, **50**, 5307–5309.
31 A. M. Laradji, C. D. McNitt, N. S. Yadavalli, V. V. Popik and S. Minko, *Macromolecules*, 2016, **49**, 7625–7631.
32 A. Poloukhtine and V. V. Popik, *J. Phys. Chem. A*, 2006, **110**, 1749–1757.
33 W. Luo, P. Gobbo, C. D. McNitt, D. A. Sutton, V. V. Popik and M. S. Workentin, *Chem. Eur. J.*, 2017, **23**, 1052–1059.
34 M. D'Abramo, M. Aschi and A. Amadei, *Chem. Phys. Lett.*, 2015, **639**, 17–22.
35 J. Yip, J. Duhamel, X. P. Qiu and F. M. Winnik, *Macromolecules*, 2011, **44**, 5363–5372.